

# Macromonomer formation by sterically hindered radical polymerization of methyl acrylate trimer at high temperature

Tomoyuki Hirano, Bunichiro Yamada\*

*Department of Applied and Bioapplied Chemistry, Graduate School of Engineering, Osaka City University, Osaka 558-8585, Japan*

Received 13 August 2002; received in revised form 17 October 2002; accepted 21 October 2002

## Abstract

Polymerization of the unsaturated trimer of methyl acrylate (MAT) was carried out by radical means at 70–130 °C. Fragmentation of propagating radicals resulting in  $\omega$ -unsaturated end groups was studied as a synthetic route to macromonomers by radical polymerization. The ratios of the propagation rate constant to the fragmentation rate constant were 7.15 and 0.94 at 50 and 130 °C, respectively. MAT polymerization at 130 °C or above is suppressed by fragmentation of the propagating radical and the low ceiling temperature to facilitate efficient introduction of the unsaturated end groups. Copolymerization between MAT and macromonomer resulted in a small amount of polymer of higher molecular weight than the main polymeric product. Homopolymerization of MAT and its copolymerization with macromonomer appear to be influenced by rapid fragmentation, which renders the addition step reversible. This mechanism would regulate the chain length of the polymer and limit further reaction of the end group. © 2002 Elsevier Science Ltd. All rights reserved.

**Keywords:** Propagation; Fragmentation; Gel-permeation chromatography

## 1. Introduction

A variety  $\alpha$ -(substituted methyl)acrylates can homopolymerize as a result of the favorable balance of sterically hindered propagation and termination as confirmed by determination of the rate constants for propagation ( $k_p$ ) and termination ( $k_t$ ) based on ESR spectroscopic quantification of propagating radical [1,2]. Slow propagation of sterically hindered monomers has also been shown by the pulsed laser polymerization method [3,4]. Another characteristic behavior of some  $\alpha$ -(substituted methyl)acrylic esters in free radical polymerization is addition–fragmentation chain transfer (AFCT) introducing the 2-carboalkoxy-2-propenyl group bound to the  $\omega$ -end of the polymer [5,6].  $\alpha$ -(Alkylthiomethyl)- [5,7,8],  $\alpha$ -(bromomethyl)- [9–12] and  $\alpha$ -(arylsulfonylmethyl)acrylates [13] are typical AFCT agents which result in the introduction of the respective  $\alpha$ -end groups together with the common carboalkoxypropenyl  $\omega$ -end group. Furthermore, some of the acrylates such as methyl  $\alpha$ -chloromethylacrylate (MCMA) [14], methyl  $\alpha$ -phenoxymethylacrylate (MPMA) [15], and  $\alpha$ -(2-carbo-

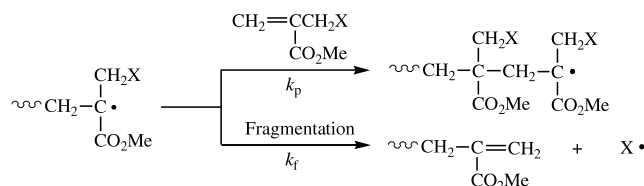
methoxyethyl)acrylate (MAD) [16] function as AFCT agents and polymerizable monomers, simultaneously.

Slow propagation arising from steric hindrance allows a certain extent of fragmentation of propagating radicals to occur as confirmed in the polymerization of MAD (Scheme 1: X = CH<sub>2</sub>CO<sub>2</sub>Me for MAD) [16]. The propenyl end group introduced does not homopolymerize, although addition of propagating radicals of common monomers to the end group is known to be feasible [6,9–11,17,18]. Polymer bearing the propenyl end group has attracted attention as a radically copolymerizable macromonomer prepared by radical polymerization. Fragmentation of propagating radicals is significantly accelerated by raising the temperature because of the higher activation energy for fragmentation than propagation [19]. Mid-chain radicals (MCRs) formed during polymerization of acrylic esters [20–23] are structurally similar to propagating radical of MAD (PMAD radical), and MCRs in acrylate polymerization at high temperature yield macromonomer [23–25]. The unsaturated trimer of methyl acrylate (MAT), a polymerizable  $\alpha$ -(substituted methyl)acrylate, yields a propagating radical (PMAT radical) with the same structure as the MCR formed by backbiting during polymerization of methyl acrylate.

In our previous paper [11], the values of  $k_p$  and  $k_t$  for

\* Corresponding author. Tel./fax: +81-6-6605-2797.

E-mail address: [yamada@chem.eng.osaka-cu.ac.jp](mailto:yamada@chem.eng.osaka-cu.ac.jp) (B. Yamada).



Scheme 1.

MAT were determined up to 60 °C, but the fragmentation behavior of the propagating radical was not examined. However, fragmentation of PMAT radical is highly expected from the behavior of the PMAD radical; the larger  $\alpha$ -substituent of the PMAT radical compared to the PMAD radical would facilitate  $\beta$ -fragmentation when  $\text{X} = \text{CH}(\text{CO}_2\text{Me})\text{CH}_2\text{CH}_2\text{CO}_2\text{Me}$  as shown in Scheme 1. In the present article,  $k_p$  and  $k_t$  values for MAT were determined over a wider temperature range than that in our previous paper [11] to reveal the details of sterically hindered propagation associated with fragmentation. We were able to accomplish efficient introduction of propenyl end groups by the AFCT mechanism based on the temperature dependence of the competition of fragmentation with propagation during homo- and copolymerization of MAT.

## 2. Experimental

### 2.1. Materials

MAT was synthesized by reaction of MA using tri(*n*-butyl)phosphine as a catalyst according to the method described for preparation of MAD [11,26], and was purified by distillation under reduced pressure: bp 110 °C/0.5 mm Hg. MA and cyclohexyl acrylate (CHA) were commercially available. Commercial 2,2'-azobis(2,4-dimethylvaleronitrile) (AVN) and 1,1'-azobis(cyclohexane-1-carbonitrile) (ACN) were recrystallized from methanol. Dimethyl 2,2'-azobis(isobutyrate) (MAIB) and 2,2'-azobis(2,4,4-trimethylpentane) (ATMP) were also commercially available and recrystallized from *n*-hexane. Commercial *tert*-butyl peroxide (TBP) was used without further purification. Solvents and other reagents were used after purification by ordinary methods.

### 2.2. Polymerization

All polymerizations were carried out in bulk at ca. 4.0 mol/l in glass tubes sealed under vacuum. After polymerization for a prescribed time, the contents of the tube were poured into a large amount of hexane to precipitate the polymeric product. Conversion of MAT was obtained by FT-near infrared spectroscopy (FT-NIR) and the overtone absorption of  $\text{C}=\text{C}-\text{H}$  stretching at  $6170\text{ cm}^{-1}$  was chosen to monitor monomer conversion. The number and weight average molecular weights ( $M_n$  and

$M_w$ ) were determined using gel-permeation chromatography (GPC). The intensity ratio of the resonances due to the unsaturated methylene group (5.5–5.7 and 6.1–6.3 ppm) to that due to the methoxy group (3.5–3.8 ppm) in  $^1\text{H}$ -NMR spectrum was employed for calculation of the  $M_n$  (NMR).

### 2.3. Measurements

FT-NIR monitoring of the polymerization was carried out in a custom-made aluminum block furnace using a Jasco INT-400 equipped with an MCT detector. A 5 mm o.d. Pyrex tube containing the polymerization mixture was degassed and sealed under vacuum. The baseline of the spectrum was determined using an empty Pyrex tube. GPC was carried out employing a Tosoh 8000 series high-performance liquid chromatograph equipped with TSK-gel columns G5000HHR, GMultiporeHXL-M, and GMHHR-L connected in this order. The molecular weight was calibrated by poly(styrene) standards.  $^1\text{H}$ - and  $^{13}\text{C}$ -NMR spectra were recorded on a JEOL JNM-A 400 spectrometer at 400 and 100 MHz, respectively. Deuteriochloroform and tetramethylsilane were used as solvent and internal standard, respectively. Electron spin resonance (ESR) spectra of propagating radicals were acquired on a Bruker ESP-300 spectrometer at the X band (9.66 GHz) with 100 kHz field modulation at a microwave power of 5.0 mW with care taken to avoid saturation. The ESR spectra were recorded at a modulation amplitude of 10.0 G after four scans over a magnetic field of 120 G width centered at 3385 G divided into 1024 points, and the conversion time and time constant were 40.96 and 655.36 ms, respectively. A 3 mm o.d. vacuum sealed quartz tube containing the monomer and initiator were maintained at the polymerization temperature in the cavity. Absolute radical concentrations were obtained by calibration using the signal from a known concentration of 2,2,6,6-tetramethylpiperidiny-1-oxyl dissolved in MAT at 40 °C. The ESR data obtained in the temperature range 70–110 °C were corrected for the effect of temperature on the ESR signal intensity [27].

## 3. Results and discussion

### 3.1. Polymerizations at different temperatures

Polymerization of MAT in the temperature range 40–60 °C has already been described in our previous paper [11]. In the present study, polymerizations mainly at higher temperatures were carried out under the conditions described in Table 1. All polymers were precipitated in hexane as viscous materials. Fig. 1a shows plots of conversion versus time obtained by gravimetry and FT-NIR revealing good agreement up to high conversion; low molecular weight polymer was not lost by precipitation using hexane.

First order kinetic plots with respect to monomer

Table 1  
Results of homopolymerization of MAT and the  $k_p$  and  $k_t$  values at different temperatures

Temperature (°C)	[Initiator] (mol/l)	$R_i \times 10^6$ (mol/l s) <sup>a</sup>	[MAT·] $\times 10^6$ (mol/l)	$k_p/k_t^{0.5}$ (l <sup>0.5</sup> /mol <sup>0.5</sup> s <sup>0.5</sup> )	$k_p$ (l/mol s)	$k_t \times 10^{-5}$ (l/mol s)
50	AVN, 0.08	1.31	4.24	0.0050	1.3	0.73
70	MAIB, 0.04	1.31	3.55	0.0107	2.9	1.04
90	ACN, 0.05	1.28	2.68	0.0151	6.4	1.78
110	ATMP, 0.06	1.27	1.82	0.0238	14.7	3.83
130	TBP, 0.02	1.29	— <sup>b</sup>	0.0265	—	—
135	TBP, 0.01	1.34	n.d.	0.0242	—	—

<sup>a</sup> Calculated from  $R_i = 2fk_d[I]$ , and efficiency of initiation ( $f$ ) = 0.5 and 1.0 for azo and peroxide initiators, respectively.

<sup>b</sup> Radical concentration was too low to be quantified by ESR spectroscopy.

according to Eq. (1) using the FT-NIR data in Fig. 1a are shown in Fig. 1b. The values of  $k_p/k_t^{0.5}$  were calculated from the slopes of the linear relationships.

$$\ln[M]_0/[M] = k_p[\text{PMAT}\cdot][\text{MAT}] = R_i^{0.5}(k_p/k_t)^{0.5}[\text{MAT}] \quad (1)$$

Although  $k_p/k_t^{0.5}$  increased with increasing temperature up to 130 °C, the value at 135 °C was lower than at 130 °C (Table 1 and Fig. 2). An increase in temperature is expected to result in a greater increase in the rate of fragmentation relative to that of propagation because of the higher activation energy of the fragmentation reaction [16]. The effect of fragmentation on the apparent value of  $k_t$  will be discussed later.  $\alpha$ -(Substituted methyl)acrylates are known to often exhibit relatively low values of  $T_c$  [28], e.g. methyl  $\alpha$ -[2,2'-bis(carbomethoxy)ethyl]acrylate [29], di-*n*-butyl itaconate [30], methyl  $\alpha$ -ethylacrylate [31], and methyl  $\alpha$ -benzylacrylate [32]. A weak dependence of the polymerization rate of MAD on the equilibrium monomer concentrations was observed as the influence of  $T_c$  [16]. Polymer formation of MAT at high temperature can thus be

anticipated to be suppressed both by fragmentation of propagating radicals and a low  $T_c$ .

The 5-line ESR spectra observed during the polymerizations of MAT were identical to those already reported, indicating a carbon centered radical coupled with two sets of two  $\beta$ -hydrogens which are almost magnetically equivalent [11]. Any resonances assignable to the expelled radical by fragmentation were not detected. The steady state concentration of PMAT radical ([PMAT·]) was obtained by double integration (Table 1). The radical concentration at 130 °C was too low to be quantified.

### 3.2. $k_p$ and $k_t$ for MAT

Values of  $k_p$  and  $k_t$  at different temperatures were obtained as functions of temperature from Eqs. (2) and (3), respectively (Table 1).

$$d(\ln[\text{MAT}]_0/[\text{MAT}])/dt = k_p[\text{PMAT}\cdot] \quad (2)$$

$$k_t = R_i/[\text{PMAT}\cdot]^2 \quad (3)$$

Fig. 3 shows the Arrhenius plots of  $k_p$  for MAT determined by the ESR method using data from this work and our previous publication [11], and  $k_p$  for MAD determined by the ESR [16] and PLP [4] methods. The activation energy ( $E_p$ ) and frequency factor for propagation ( $A_p$ ) were calculated from the linear relationships. Although the  $E_p$  values of these monomers (Table 2) are similar, the  $A_p$  value for MAT was considerably lower than for MAD.

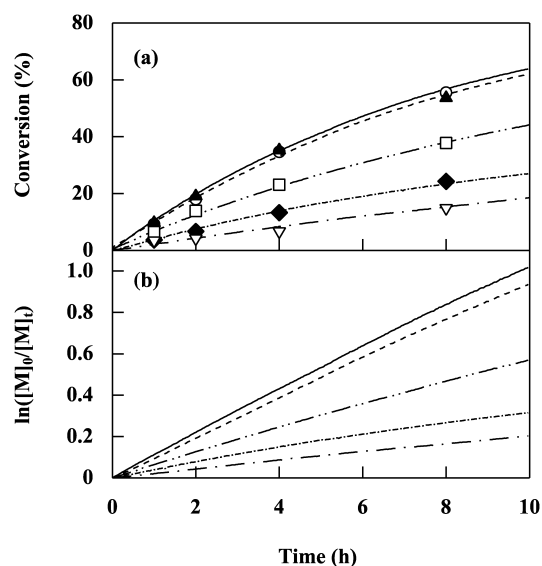


Fig. 1. Conversion-time (a) and first order (b) plots for bulk polymerization of MAT based on conversion measured by the FT-NIR method at 50 (— · — ·), 70 (— · — ·), 90 (— · — ·), 110 (— · — ·), and 130 °C (—) and by gravimetry at 50 (▽), 70 (◆), 90 (□), 110 (▲), and 130 °C (○).

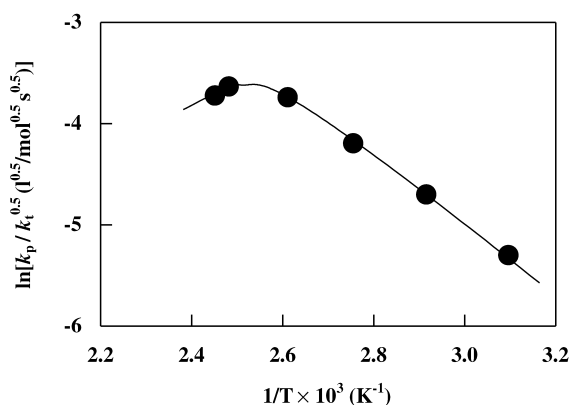


Fig. 2. Arrhenius plot of  $k_p/k_t^{0.5}$  for bulk polymerization of MAT.

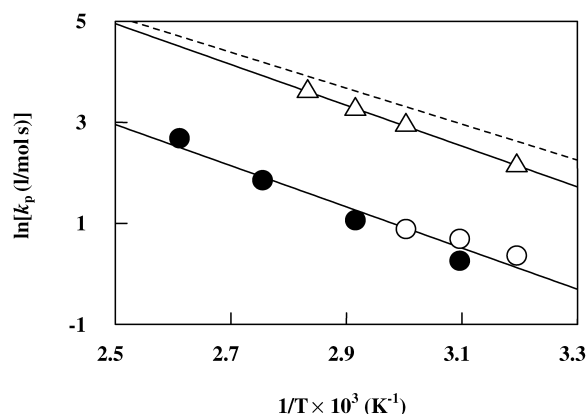


Fig. 3. Arrhenius plots of  $k_p$  for MAT based on the present work (●) and the previous work (○, Ref. [9]) and MAD (Δ, Ref. [16]). Dotted line shows the Arrhenius plot of  $k_p$  for MAD determined by the pulsed laser polymerization method (Ref. [4]).

Apparently, difference in the intercept on the ordinate rather than the slope of the linear relationship primarily explains the difference in  $k_p$  value between MAT and MAD over the temperature range shown in Fig. 3. Steric congestion around the radical center of PMAT· would result in a decrease in the  $A_p$  value.

The activation energy of termination ( $E_t$ ) for MAD is similar to that of common vinyl monomers such as St and MMA, but the frequency factor for termination ( $A_t$ ) for MAD is lower than for St and MMA:  $E_t = 6.3$  kJ/mol and  $A_t = 9.7 \times 10^6$  l/mol s for MAD,  $E_t = 8.0$  kJ/mol and  $A_t = 5.8 \times 10^7$  l/mol s for St, and  $E_t = 11.9$  kJ/mol and  $A_t = 1.1 \times 10^8$  l/mol s for MMA [33]. Congestion around the radical center is expected to lead to slow bimolecular termination of PMAD radicals [16]. Considering the greater steric hindrance in the case of MAT, we expected the value of  $A_t$  to be lower than for MAD, but did not expect any significant difference in the case of  $E_t$ . The value of  $A_t$  for MAT was greater than that for MAD by three orders of magnitude in disagreement with expectation:  $A_t = 2.2 \times 10^9$  for MAT and  $A_t = 9.7 \times 10^6$  l/mol s for MAD (Table 2). Furthermore, the value of  $E_t$  was as high as 28.1 kJ/mol for MAT, to be compared with 6.3 kJ/mol for MAD (Table 2).

A unimolecular reaction is featured by a greater activation energy and frequency factor in comparison with a bimolecular reaction when both reactions proceed at

comparable rates. The exceptionally high values of  $A_t$  and  $E_t$  for the MAT polymerization are believed to be the results of the influence of a unimolecular reaction such as fragmentation. Although the  $E_t$  value for diffusion controlled termination might be larger than the ordinary  $E_t$  value, the  $A_t$  for could not be as large as of the order of  $10^9$  l/mol s. The active radical ( $\cdot\text{CH}(\text{CO}_2\text{Me})\text{CH}_2\text{CH}_2\text{CO}_2\text{Me}$ ) expelled by fragmentation of PMAT radical at high temperatures (Scheme 2) would participate in reinitiation and termination of PMAT radical, simultaneously. The cross-termination step is predicted to be faster than mutual reaction of PMAT radicals, and the contribution of cross-termination between the active radical and PMAT radical would be to increase with increasing temperature. The temperature dependence of the apparent  $k_t$  would be stronger than that of the  $k_t$  corresponding to the 'true' bimolecular termination reaction of PMAT radicals as a result of the high activation energy of fragmentation. The  $k_t$  value obtained for MAD does not appear to be influenced by fragmentation of the propagating species.

### 3.3. Fragmentation of propagating radical

Fig. 4 shows the  $^1\text{H}$ - and  $^{13}\text{C}$ -NMR spectra of PMAT prepared at 110 °C. The main peaks can be assigned to methine and methylene protons (1.1–2.9 ppm) and the methoxy protons (3.3–4.0 ppm). The weak signals appearing at 5.5–5.7 and 6.1–6.3 ppm are attributed to the olefinic protons of the end group produced by  $\beta$ -fragmentation of PMAT radical. In the  $^{13}\text{C}$ -NMR spectrum of the polymer, the resonances ascribed to carbons of the monomeric unit and the end group can be observed: 26.0–27.0 ( $\text{CH}_2\text{--C}=\text{C}$  of end group overlapped with methyl group of *tert*-butoxy group), 47.2–48.2 (quaternary carbon of MAT unit), 51.3–52.0 (CHO), 126.8–128.5 ( $\text{CH}_2=\text{C}$ ), 136.2–137.6 ( $\text{CH}_2=\text{C}$ ), and 172.6–176.2 ppm ( $\text{C}=\text{O}$ ). Table 3 lists the  $M_n$  calculated from  $^1\text{H}$ -NMR spectral intensities ( $M_n$  (NMR)) based on the assumption that the  $\omega$ -end groups of the resultant polymers are quantitatively introduced by fragmentation of PMAT radicals as shown in Scheme 2.

Fig. 5 shows GPC elution curves of PMATs obtained at different temperatures at monomer conversion 5–10%. All the curves exhibit a major peak at 23–30 min and a minor peak at 19–23 min. The relative amount of high molecular

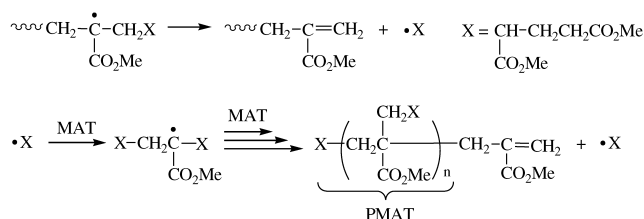
Table 2  
The values of  $E$  and  $A$  for propagation, termination and fragmentation

Monomer	Propagation		Termination <sup>a</sup>		Fragmentation		Ref.
	$E_p$ (kJ/mol)	$A_p$ (l/mol s)	$E_t$ (kJ/mol)	$A_t$ (l/mol s)	$E_f$ (kJ/mol)	$A_f$ (l/mol s)	
MAT <sup>b</sup>	33.9	$5.1 \times 10^5$	28.1	$2.2 \times 10^9$	71.5	$8.6 \times 10^{10}$	This work
MAD <sup>c</sup>	33.6	$3.4 \times 10^6$	6.3	$9.7 \times 10^6$	92.1	$3.3 \times 10^{13}$	16

<sup>a</sup>  $k_t$  for MAT and MAD at 70 °C are  $1.04 \times 10^5$  l/mol s (see Table 1) and  $4.9 \times 10^5$  l/mol s from Ref. [16], respectively.

<sup>b</sup> Temperature range of 40–110 °C.

<sup>c</sup> Temperature range of 40–80 °C.



Scheme 2.

weight material decreased with increasing temperature.  $M_n$  (NMR), calculated from the end group content of all polymeric product, was always greater than  $M_n$  (GPC) given by the main peak by a factor of 1.50–1.75. This discrepancy can be explained by bimolecular termination reactions between PMAT radicals and also between PMAT radicals and the radicals expelled by fragmentation, resulting in polymer without an unsaturated group at the  $\omega$ -end. A temperature increase favors fragmentation, and thus also termination between expelled radicals and PMAT radicals.

As mentioned earlier, the termination reaction between an expelled radical and a PMAT radical is expected to be faster than bimolecular termination of PMAT radicals; however, in spite of this the net result is that the contribution of termination reactions as end forming events decreases as the temperature is increased as manifested in slightly lower values of  $M_n$  (NMR)/ $M_n$  (GPC) (Table 3). A contributing factor to the  $M_n$  (NMR)/ $M_n$  (GPC) discrepancy may also be due to the  $M_n$  (GPC) value that could be somewhat

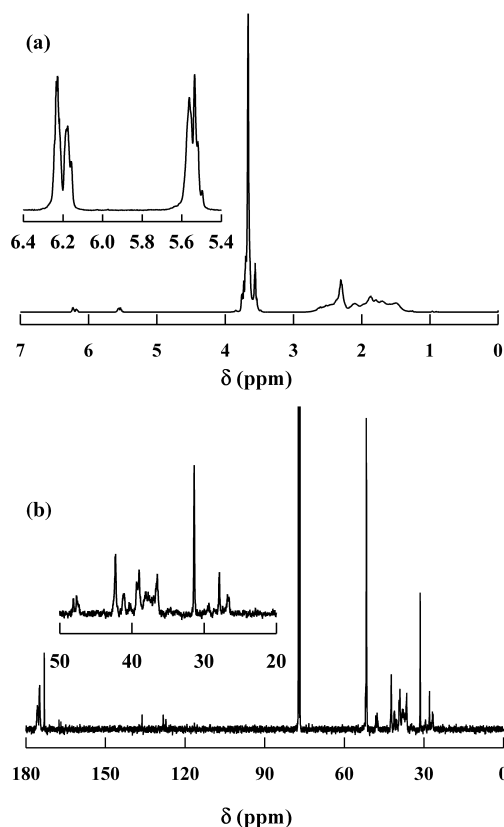
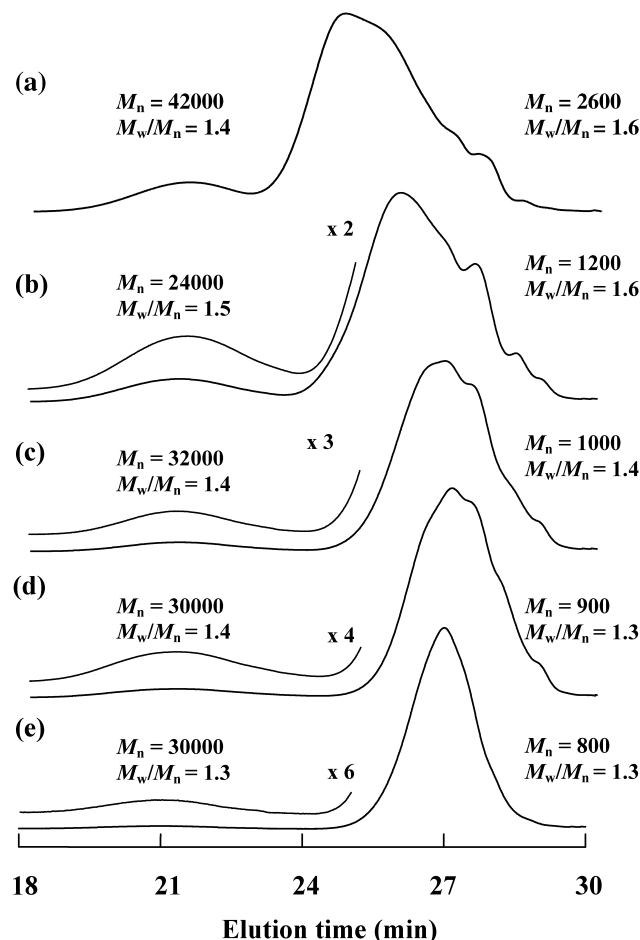
Fig. 4.  $^1\text{H}$ - and  $^{13}\text{C}$ -NMR spectra of PMAT prepared at 110 °C.

Fig. 5. GPC elution curves of PMAT prepared at 50 °C (4.2% conversion) (a), 70 °C (7.8% conversion) (b), 90 °C (5.0% conversion) (c), 110 °C (8.9% conversion) (d), and 130 °C (7.4% conversion) (e).

underestimated because of calibration with standard polystyrene, considering that PMAT has large substituents along the main chain. Separate  $M_n$  calculation from the low molecular weight peak only at 70 °C resulted in the same  $M_n$  as when using all polymer, suggesting the discrepancy between  $M_n$  (NMR) and  $M_n$  (GPC) is not specifically related to the high molecular weight peak. The peak at high molecular weight is probably resulting from copolymerization of  $\omega$ -unsaturated end groups (generated by fragmentation) with MAT.

### 3.4. $k_f$ value

The initiation rate was adjusted to be approximately constant by careful selection of initiator type and amount, and the decrease in  $M_n$  (GPC) with increasing temperature (Table 3) is mainly ascribed to acceleration of the fragmentation of PMAT radical and the effect of  $T_c$ . The ratio of [MAT unit]/[CH<sub>2</sub>=C group] was determined from the intensity ratio of the  $^1\text{H}$ -NMR resonances assigned to the protons of CH<sub>2</sub>=C and OCH<sub>3</sub> groups. The values of  $k_p/k_f$  and  $k_f$  at different temperatures calculated from Eq. (4) are



Table 3

Results of homopolymerization of MAT accompanied by fragmentation of propagating radical at different temperatures

Temperature (°C) <sup>a</sup>	$M_n$		$M_w/M_n$ (GPC)	$\frac{M_n(\text{NMR})}{M_n(\text{GPC})}$	$\frac{[\text{MAT unit}]}{[\text{CH}_2=\text{C group}]}$	$k_p/k_f$ (l/mol)	$k_f$ (s <sup>-1</sup> )
	GPC <sup>b</sup>	NMR <sup>c</sup>					
50	2600	7600	1.6	2.92	28.6	7.15	0.18
70	1200	2100	1.6	1.75	6.97	1.74	1.67
90	1000	1600	1.4	1.60	5.32	1.33	4.81
110	900	1500	1.3	1.67	4.67	1.17	12.56
130	800	1200	1.3	1.50	3.74	0.94	— <sup>d</sup>

<sup>a</sup> Polymerization conditions at the respective temperatures are given in Table 1.<sup>b</sup>  $M_n$  of polymer eluted at 23–30 min, see Fig. 5.<sup>c</sup> Calculated from <sup>1</sup>H-NMR spectral intensity ratio of the resonances due to the unsaturated end group and the methoxy group.<sup>d</sup>  $k_p$  required for  $k_f$  calculation was not available.

summarized in Table 3:

$$\frac{[\text{MAT unit}]}{[\text{CH}_2=\text{C group}]} = \frac{k_p[\text{PMAT}\cdot][\text{MAT}]}{k_f[\text{PMAT}\cdot]} = \frac{k_p[\text{MAT}]}{k_f} \quad (4)$$

The Arrhenius plot for  $k_f$  is shown in Fig. 6. The Arrhenius parameters for fragmentation ( $E_f$  and  $A_f$ ) calculated from the numerical values of  $k_f$  up to 110 °C are also summarized in Table 2. These values are compared with the corresponding values for MAD. The value of  $E_f$  is lower for MAT than for MAD; this seems reasonable considering the increased steric congestion around the radical center in the case of the PMAT radical. The lower  $E_f$  for MAT suggests that the transition state of the fragmentation of PMAT radical is closer to the reactant than that of PMAD radical according to Hammond's postulate [34]. Therefore, the value of  $A_f$  obtained for MAT appears to be somewhat low for a unimolecular reaction, indicating that bond cleavage at the transition state of the fragmentation is not sufficient as the transition state of the fragmentation of PMAD radical.

### 3.5. Reactions of end group

In relation to the reactivity of PMAT bearing the unsaturated end group as a macromonomer, copolymerization of MAT ( $M_1$ ) as a model of the end group and CHA

( $M_2$ ) was carried out in benzene at 110 °C. The values of  $r_1$  and  $r_2$  were found to be 0.54 and 0.96, respectively. The reactivity ( $1/r_2$ ) of MAT toward PCHA radical relative to CHA was 1.04, indicating that MAT is as reactive as CHA without a decrease in the reactivity by steric hindrance due to the  $\alpha$ -substituent. Consequently, the rate constants for addition of polyacrylate radicals to MAT would be of the same order as  $k_p$  for CHA [35], of the order of  $10^4$  l/mol s at 110 °C. The reactivity of CHA toward PMAT radicals relative to MAT can be evaluated as  $1/r_1 = k_{12}/k_{11} = 1.85$ . The rate constant for addition of PMAT radicals to CHA was calculated to be  $k_{12} = 27.2$  l/mol s using  $k_p$  for MAT in Table 1. Therefore, PCHA radicals readily add to MAT and CHA, while PMAT radicals add slowly to CHA and MAT. A smaller amount of higher molecular weight polymer ( $M_n = 24,000$ –42,000) together with the lower molecular weight polymer ( $M_n = 800$ –2600) as the main product can be explained by copolymerization of the unsaturated end group of PMAT or the macromonomer with MAT to consume the end group leading to an increase in  $M_n$ . MAT polymerization can be regarded to proceed via two steps as shown in Scheme 3; polymerization of MAT as the first step to give oligomer bearing the unsaturated end group (macromonomer) followed by copolymerization of the macromonomer with MAT to increase  $M_n$  up to more than 40,000.

Formation of the end group by fragmentation (rate =  $k_f[\text{PMAT}\cdot]$ ) is slower than propagation (rate =  $k_p[\text{MAT}][\text{PMAT}\cdot]$ ) by a factor of ca. 7 at 70 °C because

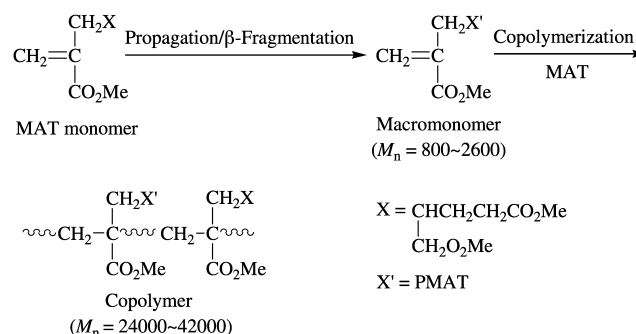
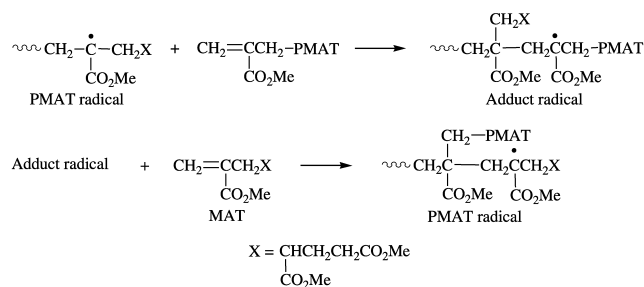


Fig. 6. Arrhenius plots for  $k_f$  of PMAT radical based on the present study (●) and the previous work (○, Ref. [9]) and PMAD radical (△, Ref. [16]).

Scheme 3.

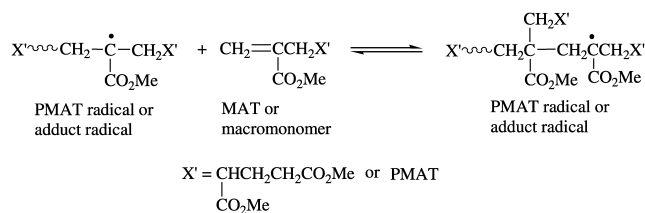


Scheme 4.

$k_p/k_t = 1.74$  l/mol as mentioned later and  $[\text{MAT}] = \text{ca. } 4$  mol/l. PMAT radicals would add to the end groups formed and to MAT to generate adduct radicals and PMAT radicals, respectively (Scheme 4). However,  $\beta$ -fragmentation of the adduct radical regenerates the end group and a PMAT radical (Scheme 5). Therefore, the reaction of the end groups with PMAT radicals is essentially reversible if the fragmentation rate of adduct radicals is comparable to the addition rate of PMAT radicals at high temperature such as  $130^\circ\text{C}$  when  $k_p/k_t = 0.94$  l/mol (Table 3). Alternatively, the reversibility can be regarded as the effect of  $T_c$  on the copolymerization. An increase in chain length would be limited by the reversible reaction of the end group leading to a narrow  $M_w/M_n$  as shown in Fig. 5. As the temperature is increased from  $50$  to  $130^\circ\text{C}$ , the polydispersities decrease from  $1.4$  to  $1.3$  and  $1.6$ – $1.3$  for the higher and lower molecular weight peaks, respectively. Actually, only an extremely small amount of high molecular weight polymer ( $M_n = 30,000$ ) and the main product of  $M_n = 800$  at  $130^\circ\text{C}$  were yielded in contrast to formation of polymer ( $M_n = 42,000$ ) and oligomer ( $M_n = 2600$ ) at  $50^\circ\text{C}$  as can be seen from Fig. 5.

#### 4. Conclusions

The large  $\alpha$ -substituent of MAT compared to that of MAD results in a smaller  $k_p$ . Competition between slow propagation arising from the steric hindrance of the bulky  $\alpha$ -substituent and  $\beta$ -fragmentation of PMAT radical leads to a decrease in  $M_n$ . Efficient introduction of the substituted propenyl  $\omega$ -end group ( $\text{CH}_2\cdot\text{C}(\text{CO}_2\text{Me})\text{CH}_2-$ ) would closely relate to suppression of polymerization at high temperature because of more significant acceleration of fragmentation than propagation with increasing temperature. Consequently, the MAT polymerization to high molecular weight was suppressed at  $130^\circ\text{C}$  or above. Although the unsaturated end group is estimated to be as reactive as CHA, the adduct radical from the end group is deduced to be much less reactive than the propagating radical of CHA. Temperature dependence of the molecular weight distributions suggests that MAT polymerization proceeds via formation of oligomeric macromonomer ( $M_n = 800$ – $2600$ ) and further copolymerization of the macromonomer with MAT to higher molecular weight



Scheme 5.

( $M_n = 24,000$ – $30,000$ ). Copolymerization of the end groups is highly suppressed, and addition of PMAT radicals to MAT and the end groups would be reversible at  $130^\circ\text{C}$  or above, thus regulating  $M_n$  and giving narrow polydispersities.

#### References

- [1] Yamada B, Kobatake S. Prog Polym Sci 1994;19:1089.
- [2] Yamada B, Westmoreland DG, Kobatake S, Konosu O. Prog Polym Sci 1999;24:565.
- [3] Yee LH, Coote ML, Chaplin RP, Davis TP. J Polym Sci Part A: Polym Chem 2000;38:2192.
- [4] Tanaka K, Yamada B, Fellows CM, Gilbert RG, Davis TP, Yee LH, Smith GB, Rees MT, Russell GT. J Polym Sci Part A: Polym Chem 2001;39:3902.
- [5] Meijs GF, Rizzardo E, Thang SH. Macromolecules 1988;21:3122.
- [6] Cacioli P, Hawthorne DG, Laslett RL, Rizzardo E, Solomon DH. J Macromol Sci Chem 1986;A23:839.
- [7] Meijs GF, Morton TC, Rizzardo E, Thang SH. Macromolecules 1991;24:3689.
- [8] Meijs GF, Rizzardo E, Thang SH. Polym Bull 1990;24:501.
- [9] Yamada B, Kobatake S. Polym J 1992;24:281.
- [10] Yamada B, Kobatake S, Aoki S. Polym Bull 1993;31:263.
- [11] Kobatake S, Yamada B. Macromol Chem Phys 1997;198:2825.
- [12] Bon SAF, Morseley SR, Waterson C, Haddleton DFM. Macromolecules 2000;33:5819.
- [13] Sato T, Seno M, Kobayashi M, Kohno T, Tanaka H. Eur Polym J 1995;31:29.
- [14] Yamada B, Kobatake S, Aoki S. Macromolecules 1993;26:5099.
- [15] Yamada B, Kobatake S, Satake M, Otsu T. J Polym Sci Part A: Polym Chem 1993;31:1551.
- [16] Kobatake S, Yamada B. J Polym Sci Part A: Polym Chem 1996;34:95.
- [17] Nair CPR, Chaumont P, Charmot D. J Polym Sci Part A: Polym Chem 1999;37:2511.
- [18] Yamada B, Oku F, Harada T. J Polym Sci Part A: Polym Chem, in press.
- [19] Fossey J, Lefort D, Sorba J. Free radicals in organic chemistry. Chichester: Wiley; 1995. p. 148.
- [20] Azukizawa M, Yamada B, Hill DJT, Pomery PJ. Macromol Chem Phys 2000;201:774.
- [21] Yamada B, Azukizawa M, Yamazoe H, Hill DJT, Pomery PJ. Polymer 2000;41:5611.
- [22] Tanaka K, Yamada B, Willemse R, van Herk AM. Polym J 2002;34:692.
- [23] Chiefari J, Jeffery J, Mayadunne RTA, Mood G, Rizzardo E, Thang SH. Macromolecules 1999;32:7700.
- [24] Chiefari J, Jeffery J, Mayadunne RTA, Mood G, Rizzardo E, Thang SH. Preparation of macromonomers via chain transfer with and without added chain transfer agent. In: Matyjaszewski K, editor. Controlled/living radical polymerization, progress in ATRP, NMP, and RAFT. ACS Symposium Series, vol. 768.; 2000. Chapter 21.

- [25] van Herk AM. *Macromol Rapid Commun* 2001;22:687.
- [26] Trumbo DL, Zander RA. *J Polym Sci Part A: Polym Chem* 1991;29:1063.
- [27] Weil JA, Bolton JR, Wertz JE. *Electron paramagnetic resonance*. New York: Wiley; 1994. p. 507.
- [28] Yamada B, Tanaka T, Otsu T. *Eur Polym J* 1989;25:117.
- [29] Kobatake S, Yamada B. *Macromolecules* 1995;28:4047.
- [30] Sato T, Inui S, Tanaka H, Ota T, Kamachi M, Tanaka K. *J Polym Sci Part A: Polym Chem* 1987;25:637.
- [31] Penelle J, Collot J, Rufford G. *J Polym Sci Part A: Polym Chem* 1993;31:2407.
- [32] Madruga EL, Roman JS, Angeles M, Moreal MCF. *Macromolecules* 1984;17:989.
- [33] Odian G. *Principles of polymerization*, 3rd ed. New York: Wiley; 1991. p. 275.
- [34] Fossey J, Lefort D, Sorba J. *Free radicals in organic chemistry*. Chichester: Wiley; 1995. p. 52.
- [35] Mukai T, Yamada B. To be published.